Electronic Supplementary Material (ESI) for Journal of Materials Chemistry A

Highly Efficient Organic Solar Cells Using Solution-Processed Active Layer with Small Molecule Donor and Pristine Fullerene

Hao-Wu Lin,[a] Jung-Hao Chang,[a] Wei-Ching Huang,[a] Yu-Ting Lin,[a] Li-Yen Lin,[b] Francis Lin,[b] Ken-Tsung Wong,*[b,c] Hsiao-Fang Wang,[d] Rong-Ming Ho[d] and Hsin-Fei Meng[e]*

[a]Department of Materials Science and Engineering, National Tsing Hua University, No. 101, Section 2, Kuang-Fu Road, Hsinchu, Taiwan 30013.
[b]Department of Chemistry, National Taiwan University, [c]Institute of Atomic and Molecular Sciences, AcademiaSinica, No.1, Section 4, Roosevelt Road, Taipei, Taiwan 10617.
[d]Department of Chemical Engineering, National Tsing Hua University, Hsinchu, Taiwan 30013.
[e]Institute of Physics, National Chiao Tung University, Hsinchu, Taiwan 30013.

Supporting Information

Contents page

Device characteristics of DP6DCTP:PC_{61}BM solar cells using spin-coating process with different structures:

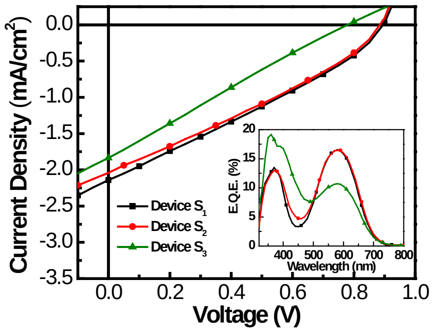

Figure S1. *J*–V characteristics (under 1 sun, AM1.5G illumination) and EQE spectra (inset) of BHJ solar cells based on a **DP6DCTP**:PC_{61}BM (1:1 by weight, 40 nm) active layer with different structures.

Table S1. Photovoltaic parameters of BHJ solar cells based on a **DP6DCTP**:PC_{61}BMactive layer with different structures under AM 1.5G simulated solar illumination at an intensity of 100 mW/cm^2.

Device type[a, b]	V_{OC} (V)	J_{SC} (mA/cm^2)	FF (%)	η (%)
Device S_1: active layer/Ag	0.90	2.1	29	0.56
Device S_2: active layer/BCP (10 nm)/Ag	0.89	2.0	30	0.55
Device S_3: active layer/C_{60} (10 nm)/BCP (10 nm)/Ag	0.78	1.8	25	0.35

[a]ITO/MoO_3 (30 nm) was used as anodes. [b]Active-layer thin films were cast from chloroform solution.

Device characteristics of DTDCTP:PC_{71}BM solar cells with different active layer thicknesses using spin-coating process:

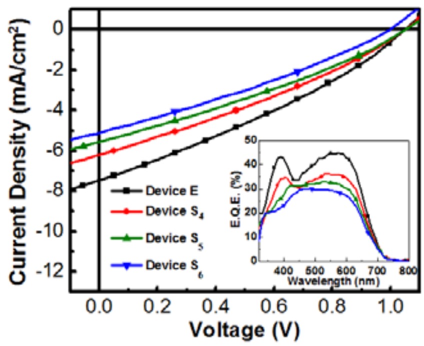

Figure S2. *J*–V characteristics (under 1 sun, AM1.5G illumination) and EQE spectra (inset) of inverted BHJ solar cells based on a **DTDCTP**:PC_{71}BM(1:2 by weight) active layer with different thicknesses.

Table S2. Photovoltaic parameters of inverted BHJ solar cells based on a **DTDCTP**:PC_{71}BM active layer with different thicknesses under AM 1.5G simulated solar illumination at an intensity of 100 mW/cm^2.

Device type[a, b]	V_{OC} (V)	J_{SC} (mA/cm^2)	FF (%)	η (%)
Device E: **DTDCTP**:PC_{71}BM (50 nm)	1.1	7.5	30	2.4
Device S_4: **DTDCTP**:PC_{71}BM (54 nm)	1.1	6.2	30	2.0
Device S_5: **DTDCTP**:PC_{71}BM (61 nm)	1.1	5.6	30	1.8
Device S_6: **DTDCTP**:PC_{71}BM (70 nm)	1.0	5.2	30	1.5

[a]ITO/Ca (1 nm)/**DTDCTP**:PC_{71}BM/**DTDCTP** (7 nm)/MoO_3 (7 nm)/Ag. [b]Active-layer thin films were cast from chlorobenzene solution.

Device characteristics of DTDCTP:C_{70} solar cells with different active layer thicknesses using spin-coating process:

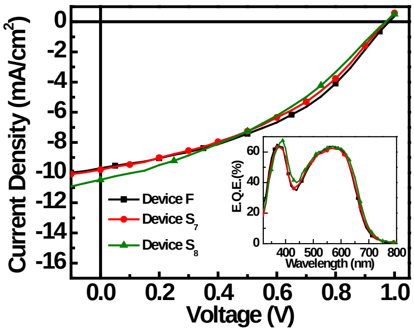

Figure S3. *J*–V characteristics (under 1 sun, AM1.5G illumination) and EQE spectra (inset) of inverted BHJ solar cells based on a **DTDCTP**:C_{70}(1:1.5 by weight) active layer with different thicknesses.

Table S3. Photovoltaic parameters of inverted BHJ solar cells based on a **DTDCTP**:C_{70} active layer with different thicknesses under AM 1.5G simulated solar illumination at an intensity of 100 mW/cm^2.

Device type[a, b]	V_{OC} (V)	J_{SC} (mA/cm^2)	FF (%)	η (%)
Device F: **DTDCTP**:C_{70} (50 nm)	0.98	9.7	42	4.0
Device S_7: **DTDCTP**:C_{70} (54 nm)	0.97	9.8	40	3.8
Device S_8: **DTDCTP**:C_{70} (61 nm)	0.97	10.5	36	3.5

[a]ITO/Ca (1 nm)/**DTDCTP**:C_{70}/**DTDCTP** (7 nm)/MoO_3 (7 nm)/Ag. [b]Active-layer thin films were cast from DCB solution.

Device characteristics of DPDCPB:C_{70} solar cells with different ratios using spin-coating process:

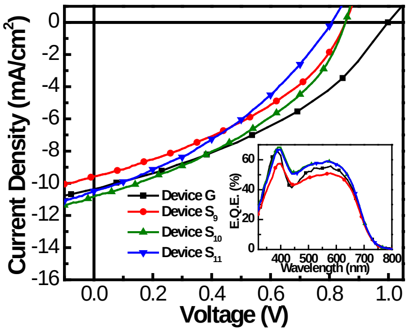

Figure S4. *J*–V characteristics (under 1 sun, AM 1.5G illumination) and EQE spectra (inset) of solar cells fabricated from **DPDCPB** and C_{70} with different blend ratios from 1:1.5 to 1:2.2(**Device G~S_{11}**).

Table S4. Performance parameters of the optimized devices under AM 1.5G simulated solar illumination at an intensity of 100 mW/cm^2.

Device type[a]	V_{OC} (V)	J_{SC} (mA/cm^2)	FF (%)	η (%)
Device G: DPDCPB:C_{70} (1:1.5)	1.01	10.9	40	4.1
Device S_9: DPDCPB:C_{70} (1:1.8)	0.83	9.1	38	2.9
Device S_{10}: DPDCPB:C_{70} (1:2.0)	0.88	8.9	38	2.9
Device S_{11}: DPDCPB:C_{70} (1:2.2)	0.63	9.6	40	2.4

[a]Active-layer thin films were cast from DCB solution by spin-coating process.

Electronic Supplementary Material (ESI) for Journal of Materials Chemistry A
This journal is © The Royal Society of Chemistry 2014

Device characteristics of DTDCPB:C_{70} solar cells with different ratios using spin-coating process:

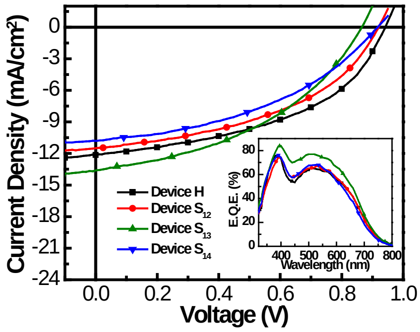

Figure S5. *J*–V characteristics (under 1 sun, AM 1.5G illumination) and EQE spectra (inset) of solar cells fabricated from **DTDCPB** and C_{70} with different blend ratios from 1:1.5 to 1:2.2(**Device H~S_{14}**).

Table S5. Performance parameters of the optimized devices under AM 1.5G simulated solar illumination at an intensity of 100 mW/cm^2.

Device type[a]	V_{OC} (V)	J_{SC} (mA/cm^2)	FF (%)	η (%)
Device H: DTDCPB:C_{70} (1:1.5)	0.94	12.1	47	5.4
Device S_{12}: DTDCPB:C_{70} (1:1.8)	0.92	11.5	45	4.8
Device S_{13}: DTDCPB:C_{70} (1:2.0)	0.87	13.6	42	5.0
Device S_{14}: DTDCPB:C_{70} (1:2.2)	0.92	10.8	42	4.1

[a]Active-layer thin films were cast from DCB solution by spin-coating process.

Device characteristics of DPDCTB:C_{70} solar cells with different ratios using spin-coating process:

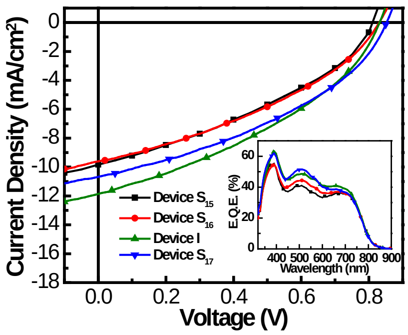

Figure S6. *J*–V characteristics (under 1 sun, AM 1.5G illumination) and EQE spectra (inset) of solar cells fabricated from **DPDCTB** and C_{70} with different blend ratios from 1:1.5 to 1:2.2 (**Device S_{15}~S_{17}**).

Table S6. Performance parameters of the optimized devices under AM 1.5G simulated solar illumination at an intensity of 100 mW/cm^2.

Device type[a]	V_{OC} (V)	J_{SC} (mA/cm^2)	FF (%)	η (%)
Device S_{15}: DPDCTB:C_{70} (1:1.5)	0.81	9.8	35	2.9
Device S_{16}: DPDCTB:C_{70} (1:1.8)	0.83	9.6	37	2.9
Device I: DPDCTB:C_{70} (1:2.0)	0.83	11.9	37	3.7
Device S_{17}: DPDCTB:C_{70} (1:2.2)	0.85	10.7	39	3.5

[a]Active-layer thin films were cast from DCB solution by spin-coating process.

Device characteristics of DTDCTB:C_{70} solar cells with different ratios using spin-coating process:

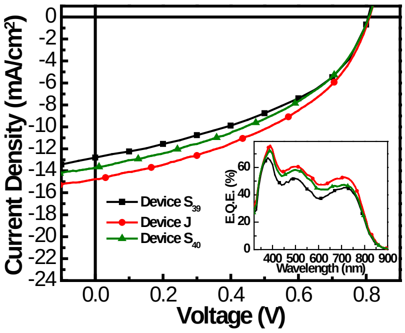

Figure S7. *J*–V characteristics (under 1 sun, AM 1.5G illumination) and EQE spectra (inset) of solar cells fabricated from **DTDCTB** and C_{70} with different blend ratios from 1:1.5 to 1:2.0 (**Device S_{18}~S_{19}**).

Table S7 Performance parameters of the optimized devices under AM 1.5G simulated solar illumination at an intensity of 100 mW/cm^2.

Device type[a]	V_{OC} (V)	J_{SC} (mA/cm^2)	FF (%)	η (%)
Device S_{18}: DTDCTB:C_{70} (1:1.5)	0.81	12.79	43	4.47
Device J: DTDCTB:C_{70} (1:1.8)	0.81	14.77	43	5.20
Device S_{19}: DTDCTB:C_{70} (1:2.0)	0.81	13.71	42	4.69
DTDCTB:C_{70} (1:2.2)[b]	-	-	-	-

[a]Active-layer thin films were cast from DCB solution by spin-coating process. [b]Poor film quality.

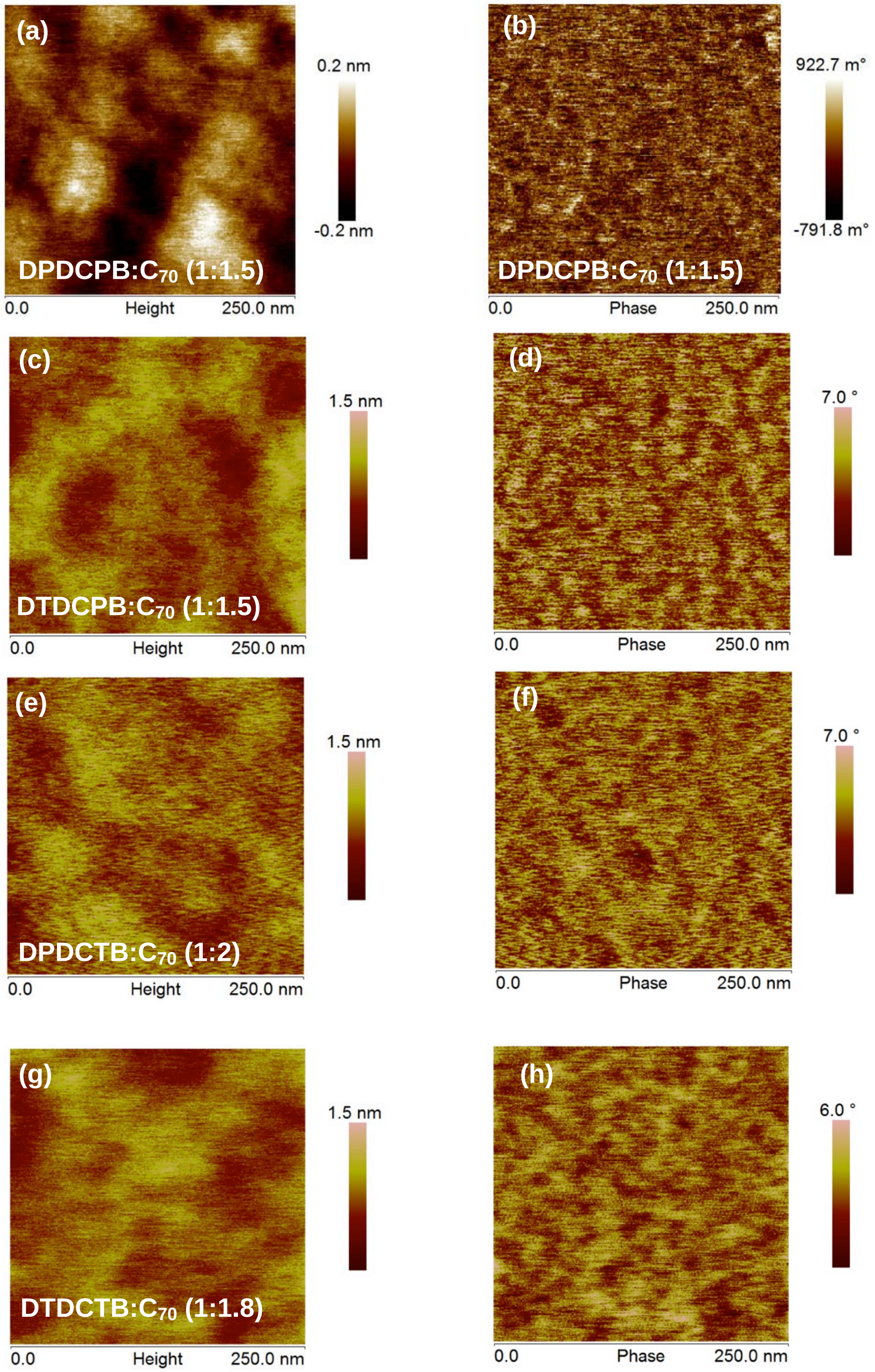

Figure S8. AFM topology and phase images of (a)(b) **DPDCPB**:C_{70} (1:1.5) thin-film, (c)(d) **DTDCPB**:C_{70} (1:1.5) thin-film, (e)(f) **DPDCTB**:C_{70} (1:2) thin-film, (g)(h) **DTDCTB**:C_{70} (1:1.8) thin-film. The thin-films were spin-coated on ITO/Ca (1 nm).

Device characteristics of DPDCPB:C_{70} solar cells with different active layer thicknesses using bar-coating process:

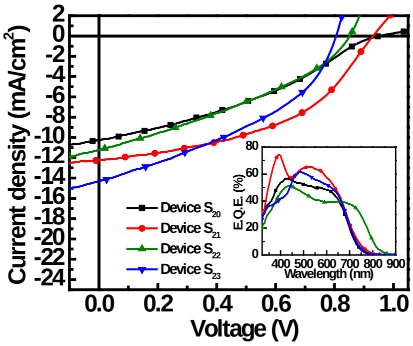

Figure S9. *J*–V characteristics (under 1 sun, AM1.5G illumination) and EQE spectra (inset) of inverted BHJ solar cells based on a **DPDCPB**:C_{70}(1:2.2 by weight) active layer with different thicknesses. The device structures are: ITO/Ca (1 nm)/**DPDCPB**:C_{70}/**DPDCPB** (7 nm)/MoO_3 (7 nm)/Ag (120 nm).

Table S8. Photovoltaic parameters of inverted BHJ solar cells based on a **DPDCPB**:C_{70}active layer with different thicknesses under AM 1.5G simulated solar illumination at an intensity of 100 mW/cm^2.

Device type[a]	V_{OC} (V)	J_{SC} (mA/cm^2)	FF (%)	η (%)
Device S_{20}: DPDCPB:C_{70} (44 nm)	0.95	10.1	34	3.3
Device S_{21}: DTDCPB:C_{70} (44 nm)	0.93	12.2	47	5.3
Device S_{22}: DPDCTB:C_{70} (44 nm)	0.85	11.2	34	3.3
Device S_{23}: DTDCTB:C_{70} (58 nm)	0.81	14.3	39	4.5

[a]Active-layer thin films were cast from DCB solution by bar-coating process.

Device characteristics of DTDCPB:C_{70} solar cells with different concentrations of 1,2,4-trichlorobenzeneusing bar-coating process:

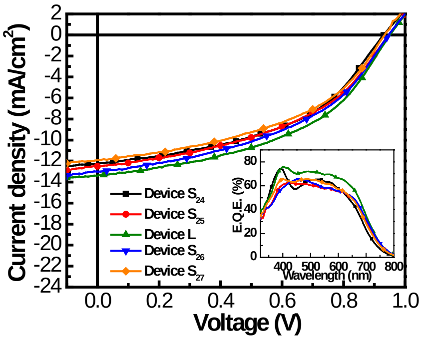

Figure S10. *J*–V characteristics (under 1 sun, AM1.5G illumination) and EQE spectra (inset) of inverted BHJ solar cells based on a **DTDCPB**:C_{70}(1:2.2 by weight) active layer without or with different concentrations of 1,2,4-trichlorobenzene (TCB).The device structures are: ITO/Ca (1 nm)/**DTDCPB**:C_{70}/**DTDCPB** (7 nm)/MoO_3 (7 nm)/Ag (120 nm).

Table S9. Photovoltaic parameters of inverted BHJ solar cells based on a **DTDCPB**:C_{70} active layer without or with different concentrations of TCB under AM 1.5G simulated solar illumination at an intensity of 100 mW/cm^2.

DTDCPB:C_{70}[a]	V_{OC} (V)	J_{SC} (mA/cm^2)	FF (%)	η (%)
Device S_{24}:1:2.2	0.93	12.2	47	5.3
Device S_{25}:1:2.2 with 20% TCB	0.95	12.5	45	5.3
Device L:1:2.2 with 50% TCB	0.95	13.4	46	5.9
Device S_{26}:1:2.2 with 80% TCB	0.94	13.2	43	5.5
Device S_{27}:1:2.2 with 100% TCB	0.93	11.9	45	5.0

[a]Active-layer thin films were cast from DCB solution without or with different concentrations of TCB by bar-coating process.

Device characteristics of DPDCTB:C_{70} solar cells with different concentrations of chlorobenzene using bar-coating process:

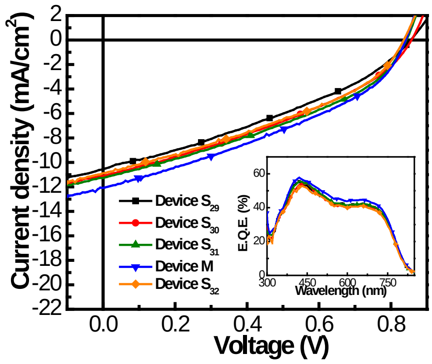

Figure S11. *J*–V characteristics (under 1 sun, AM1.5G illumination) and EQE spectra (inset) of inverted BHJ solar cells based on a **DPDCTB**:C_{70}(1:2.2 by weight) active layer without or with different concentrations of chlorobenzene (CB).The device structures are: ITO/Ca (1 nm)/ **DPDCTB**:C_{70}/ **DPDCTB** (7 nm)/MoO_3 (7 nm)/Ag (120 nm).

Table S10. Photovoltaic parameters ofinverted BHJ solar cells based on a **DPDCTB**:C_{70} active layer without or with different concentrations of TCB under AM 1.5G simulated solar illumination at an intensity of 100 mW/cm^2.

DPDCTB:C_{70}[a]	V_{OC} (V)	J_{SC} (mA/cm^2)	FF (%)	η (%)
Device S_{28}:1:2.2	0.86	10.6	33	3.1
Device S_{29}:1:2.2 with 15% CB	0.86	11.1	35	3.3
Device S_{30}:1:2.2 with 20% CB	0.84	11.3	37	3.5
Device M:1:2.2 with 30% CB	0.85	12.1	37	3.8
Device S_{31}:1:2.2 with 35% CB	0.84	10.9	36	3.3

[a]Active-layer thin films were cast from DCB solution without or with different concentrations of CB by bar-coating process.

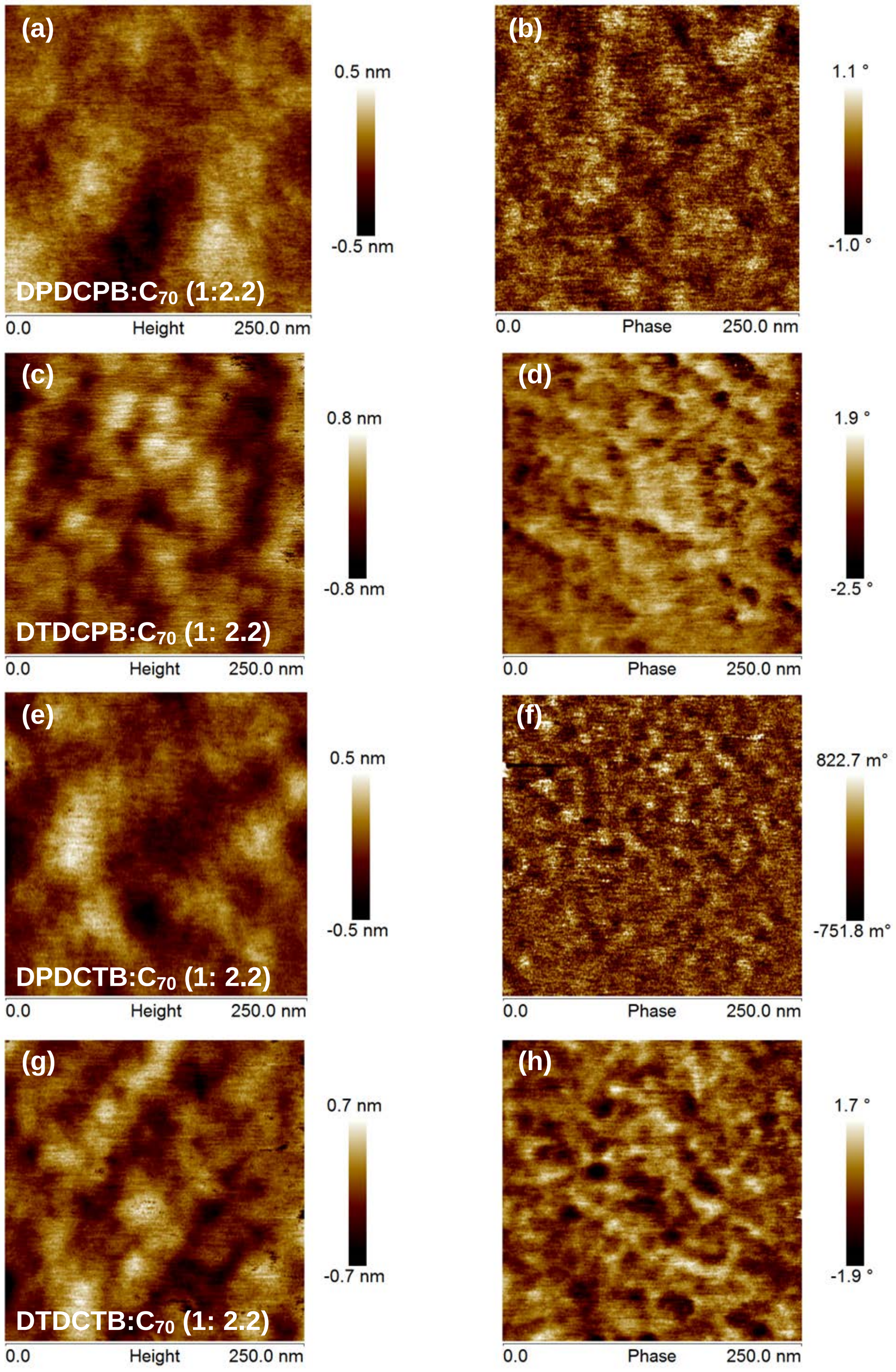

Figure S12. AFM topology (left) and phase (right) images of (a)(b) **DPDCPB**:C_{70} (1:2.2) thin-film, (c)(d) **DTDCPB**:C_{70} (1: 2.2) thin-film and (e)(f) **DPDCTB**:C_{70} (1: 2.2) thin-film and (g)(h) **DTDCTB**:C_{70} (1: 2.2) thin-film. The thin-films were bar-coated on ITO/Ca (1 nm).

TEM bright-field top-view images of DTDCPB:C_{70} with different coating methods:

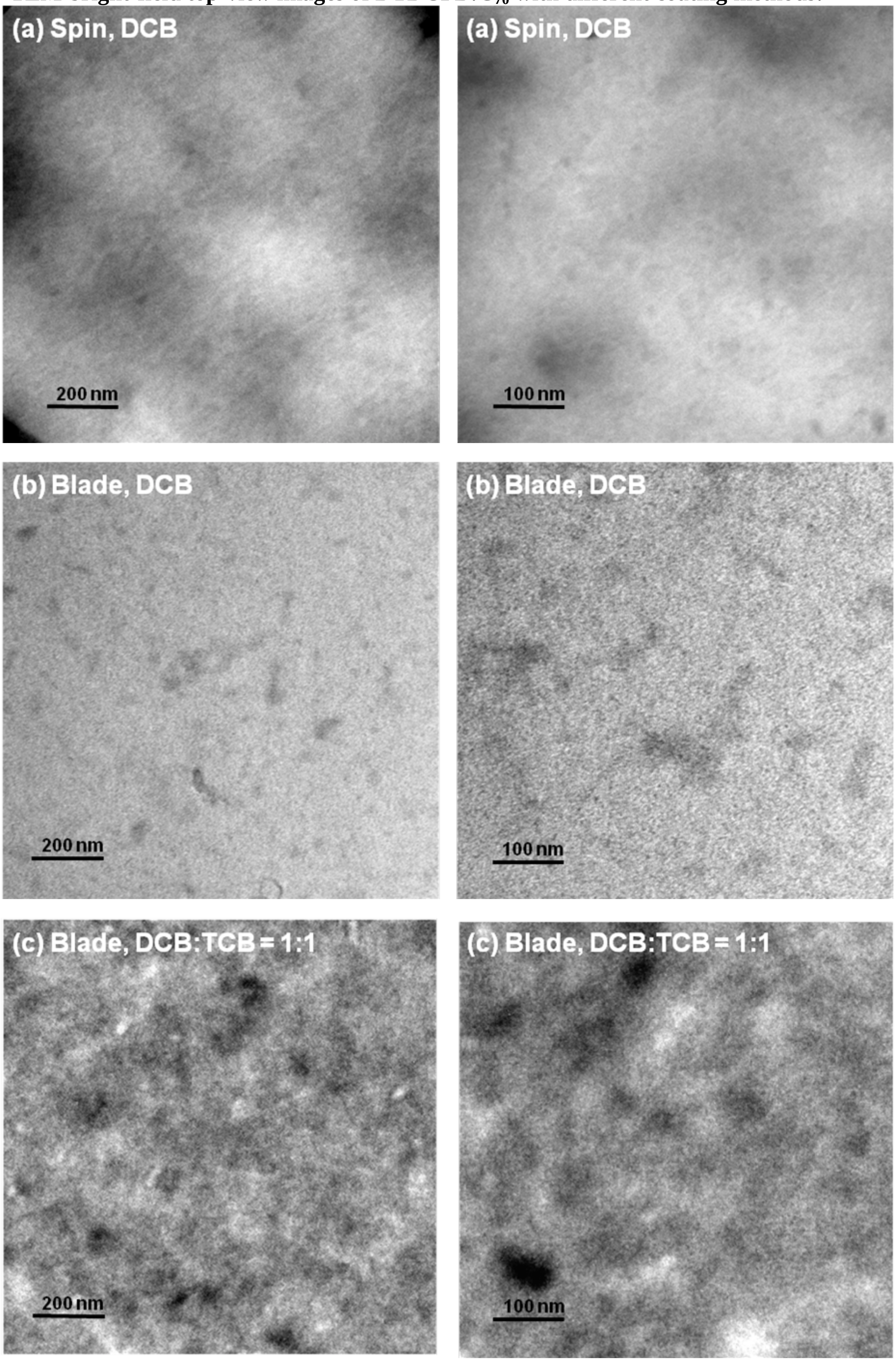

Figure S13. TEM images of (a) DTDCPB:C_{70} (1:1.5) thin film casted from 1,2-dicholorobenzene solution by spin-coated process, (b) DTDCPB:C_{70} (1:2.2) thin film casted from 1,2-dicholorobenzene solution by bar-coated process, and (c) DTDCPB:C_{70} (1:2.2) thin film casted from 1,2-dichlorobenzene and 1,2,4-trichlorobenzene (1:1 by volume) mixed solutions by bar-coated process.

Synthesis of DP6DCTP:

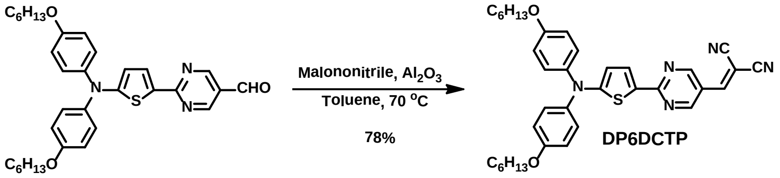

Synthesis of 2-{[2-(5-*N*,*N*-bis(4-hexyloxyphenyl)aminothiophen-2-yl)-pyrimidin-5 -yl]methylene}malononitrile(DP6DCTP). A mixture of 2-[5-*N*,*N*-bis(4-hexyloxyphenyl)aminothiophen-2-yl]-pyrimidine-5-carbaldehyde[1] (2.23 g, 4.00 mmol), malononitrile (528 mg, 8.00 mmol), and basic aluminum oxide (2.00 g) in dry toluene (60 mL) was stirred and heated at 70 °C for 2 h. After the reaction mixture was cooled to room temperature, the basic aluminum oxide residue was removed by filtration and thoroughly washed with toluene. The solvent of the filtrate was removed by rotary evaporation, and the crude product was purified by column chromatography on silica gel with dichloromethane as eluent to afford **DP6DCTP** as a dark red solid (1.90 g,78%), mp 86 °C (DSC); ^{1}H NMR (CD_2Cl_2, 400 MHz)δ8.89 (s, 2H), 7.88 (d, *J* = 4.4 Hz, 1H), 7.50 (s, 1H), 7.25 (dd, *J* = 2.4, 6.8 Hz, 4H), 6.91 (dd, *J* = 2.4, 6.8 Hz, 4H), 6.25 (d, *J* = 4.4 Hz, 1H), 3.96 (t, *J* = 6.8 Hz, 4H), 1.79 (m, 4H), 1.46 (m, 4H), 1.36 (m, 8H), 0.93 (m, 6H); ^{13}C NMR ($CDCl_3$, 100 MHz) δ165.9, 162.9, 158.2, 157.5, 152.6, 138.5, 135.5, 127.0, 125.7, 119.6, 115.5, 113.8, 113.0, 111.3,79.6, 68.3, 31.7,29.3, 25.8, 22.7, 14.2;HRMS (*m/z*, FAB^{+}) calcd. for $C_{36}H_{39}N_5O_2S$ 605.2824, found 605.2822; λ_{abs} = 564 nm (ε = 53700 M^{-1} cm^{-1}).

[1] L.-Y.Lin, C.-H.Tsai, K.-T.Wong, T.-W.Huang, C.-C.Wu, S.-H.Chou, F. Lin, S.-H.Chen and A.-I.Tsai, *J. Mater. Chem.*,2011,**21**, 5950.